KamLAND: PRESENT STATUS AND FUTURE PROSPECTS

K. Nakajima
for the KamLAND Collaboration
Research Center for Neutrino Science, Tohoku University,
Sendai 980-8578, Japan

Abstract

KamLAND is a low energy neutrino detector with 1 kton of ultra-pure liquid scintillator. The latest results of measurement of neutrino oscillation parameters based on a 766 ton-year exposure to $\overline{\nu}_{\mathrm{e}}$'s from distant nuclear reactors showed that the observed energy spectrum preferred the distortion expected from $\overline{\nu}_{\mathrm{e}}$ oscillation effects. A two-neutrino oscillation analysis determined Δm^2 precisely; $\Delta m^2 = 7.9^{+0.6}_{-0.5} \times 10^{-5}\mathrm{eV}^2$. Moreover, KamLAND announced investigation of geoneutrinos, which are generated deep inside of the earth. The measurement was consistent with current geophysical models and provided a new window for the exploration of the Earth. At present, further improvements of the sensitivity of the KamLAND detector for the real-time measurement of the low energy solar neutrinos as ^{7}Be solar neutrinos are being made.

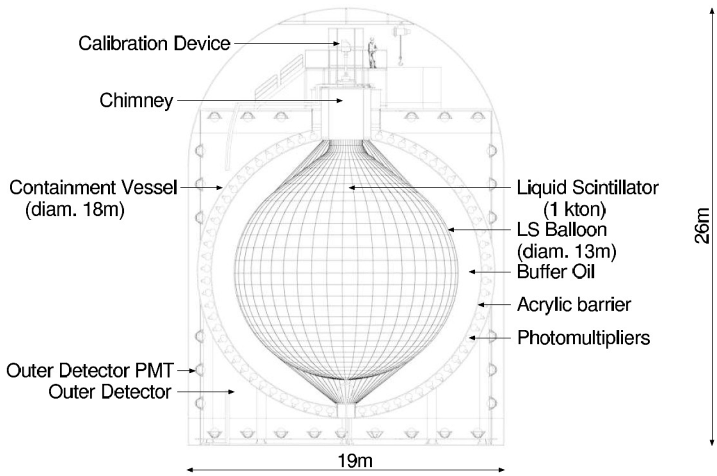

Figure 1: Schematic diagram of the KamLAND detector

1 The KamLAND experiment

The *Kam*ioka *L*iquid scintillator *A*nti-*N*eutrino *D*etector (KamLAND) is a low energy neutrino detector located in a 1000 m underground on the Kamioka Mine in Gifu Prefecture, Japan. Primary subjects of the KamLAND experiment are measurement of neutrino oscillation using reactor $\overline{\nu}_e$'s with a long baseline, detection of terrestrial antineutrinos (geoneutrinos), observation of low energy solar neutrinos, and so on. The central part of the detector is 1 kton of ultra-pure liquid scintillator surrounded by 1879 17/20-inch-diameter photomultiplier tubes (PMTs). The liquid scintillator consists of 80% dodecane, 20% pseudocumene (1,2,4-trimethylbenzene), and 1.52 g/liter of PPO (2,5-diphenyloxazole). The effective equilibrium concentrations of ^{238}U and ^{232}Th in the liquid scintillator are $(3.5 \pm 0.5) \times 10^{-18}$g/g and $(5.2 \pm 0.8) \times 10^{-17}$g/g, respectively. Although, at the beginning of the experiment, only 1325 17-inch PMTs were used corresponding to the energy resolution of $7.3\%/\sqrt{E(\mathrm{MeV})}$, since 27 February 2003, 554 20-inch PMTs have been also utilized. The photocathode coverage is 34% and the energy resolution is $6.2\%/\sqrt{E(\mathrm{MeV})}$. The shielding of 2700 m.w.e. of rock provides 0.34 Hz of cosmic-ray muons in the detector. The detector was completed in January 2002, and the measurement

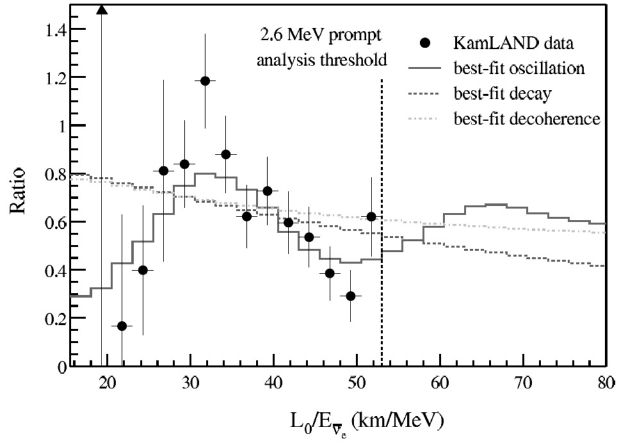

Figure 2: Ratio of the observed $\overline{\nu}_e$ spectrum to the expectation for no-oscillation versus L_0/E [2]. The data points and models are plotted with $L_0 = 180$km.

started. The first results of KamLAND in 2003 showed the disappearance of reactor $\overline{\nu}_e$'s [1]. After that, the KamLAND experiment announced the results of reactor $\overline{\nu}_e$ oscillation [2] and geoneutrinos [3] based on a total detector live time of (515.1 ± 0.3) days and (749.1 ± 0.5) days, respectively. Moreover, a high sensitivity search for $\overline{\nu}_e$'s from the sun and the other sources [4] and search for the invisible decay of neutrons [5] were carried out.

2 Measurement of reactor antineutrino oscillation

Reactor $\overline{\nu}_e$'s are detected via inverse β-decay, $\overline{\nu}_e + \mathrm{p} \rightarrow \mathrm{e}^+ + \mathrm{n}$, with a 1.8 MeV $\overline{\nu}_e$ energy threshold. In a 766 ton-year exposure of KamLAND between March 9 2002 and January 11 2004, 258 $\overline{\nu}_e$ candidate events with $\overline{\nu}_e$ energies above 3.4 MeV were observed, which include 17.8 ± 7.3 expected background events. The radial fiducial volume cut was 5.5 m, corresponding 543.7 tons of the fiducial mass (4.61×10^{31} free target protons). The event selection cuts for the time difference (ΔT) and position difference (ΔR) between the positron and delayed neutron were $0.5\mu\mathrm{s} < \Delta T < 1000\mu\mathrm{s}$ and $\Delta R < 2$m, respectively. The event energies were required to be $2.6\mathrm{MeV} < E_{\mathrm{prompt}} < 8.5\mathrm{MeV}$ and

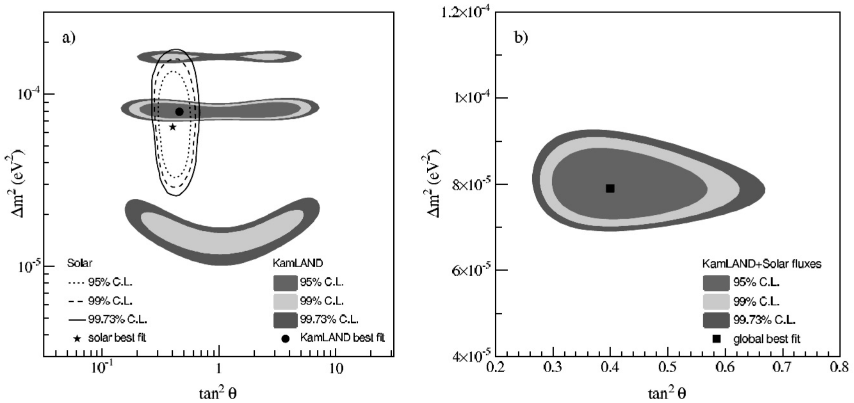

Figure 3: (a)Neutrino oscillation parameter allowed region [2]. (b)Result of a combined two-neutrino oscillation analysis of KamLAND and observed solar-neutrino fluxes under the assumption of CPT invariance [2].

1.8MeV $< E_{\text{delayed}} <$ 2.6MeV. The efficiency of all cuts was found to be $(89.8 \pm 1.5)\%$. In order to suppress backgrounds of ^{9}Li and ^{8}He spallation products, after well tracked muons passing through the detector, a 3 m radius cylinder around the track was vetoed for 2 s. For muons that produce more than $\sim 10^6$ photoelectrons above minimum ionization or muons tracked with poor reliability, the entire volume was vetoed for 2 s. The dead time introduced by all muon cuts was $(9.7\pm0.1)\%$; the total live time was (515.1 ± 0.3) days. The most dominant source of background events was $^{13}\mathrm{C}(\alpha,\mathrm{n})^{16}\mathrm{O}$ reaction in the liquid scintillator. Near 6 and 4.4 MeV, two peaks were appeared from decays of levels in ^{16}O and from γ decays following neutron inelastic scattering on ^{12}C, respectively. In the analysis region, the number of expected background events from the $^{13}\mathrm{C}(\alpha,\mathrm{n})^{16}\mathrm{O}$ reaction was 10.3 ± 7.1. On the other hand, the operation data of 53 Japanese reactors surrounding KamLAND were traced to calculate fission rates of each fissile isotope. The integrated thermal power flux over the detector live time was 701J/cm^2. The expected number of $\overline{\nu}_{\mathrm{e}}$ events was 365.2 ± 23.7(syst) assuming no $\overline{\nu}_{\mathrm{e}}$ oscillation. The combined systematic uncertainty was 6.5%. The deficit of observed neutrino events confirmed $\overline{\nu}_{\mathrm{e}}$ disappearance at the 99.998% significance level. The observed energy spectrum disagreed with the expected spectral shape in the absence of $\overline{\nu}_{\mathrm{e}}$ oscillation at 99.6%

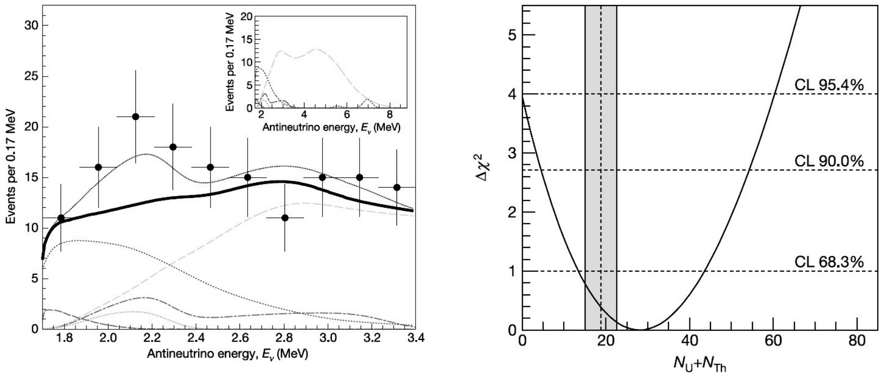

Figure 4: (Left) Electron antineutrino energy spectra in KamLAND [3]. Data points show energy distribution of 152 observed $\overline{\nu}_e$ candidates. Also shown are the expected signals from ^{238}U (dot-dashed red line) and ^{232}Th (dotted green line) geoneutrinos, and the total expected spectrum excluding the geoneutrino signal (thick solid black line) due to the backgrounds (dashed light blue line, dotted brown line and dashed purple line), and the total expectation (thin black line). (Right) Confidence intervals for the number of observed geoneutrinos [3]. Assuming the mass ratio, Th/U=3.9, the 90% confidence interval for the total number of ^{238}U and ^{232}Th geoneutrino candidates is estimated to be 4.5 to 54.2. The grey band shows the number of ^{238}U and ^{232}Th geoneutrinos predicted by the geophysical model. The KamLAND results are consistent with the prediction.

significance. The L_0/E distribution of the observed energy spectrum is shown in Figure 2. The data prefer the distortion expected from $\overline{\nu}_e$ oscillation effects. A two-neutrino oscillation analysis of the KamLAND data gave a mass-squared difference $\Delta m^2 = 7.9^{+0.6}_{-0.5} \times 10^{-5}\text{eV}^2$ and a mixing angle $\tan^2\theta = 0.46$. The best-fit point of Δm^2 was determined precisely and it is in the region commonly characterized as "LMAI". Assuming CPT invariance, a combined analysis of data from KamLAND and solar neutrino experiments yielded $\Delta m^2 = 7.9^{+0.6}_{-0.5} \times 10^{-5}\text{eV}^2$ and $\tan^2\theta = 0.40^{+0.10}_{-0.07}$. To reduce the systematic uncertainties, full-volume source calibrations have been performed in KamLAND.

3 Experimental investigation of geoneutrinos

KamLAND has the sensitivity to detect $\overline{\nu}_e$'s generated from decay chains of radiogenic nuclides of ^{238}U and ^{232}Th within the Earth (geoneutrinos). Most of the geoneutrinos are produced from ^{238}U, ^{232}Th and ^{40}K;

$$^{238}\mathrm{U} \rightarrow {}^{206}\mathrm{Pb} + 8^4\mathrm{He} + 6\mathrm{e}^- + 6\overline{\nu}_\mathrm{e} + 51.7\mathrm{MeV},$$
$$^{232}\mathrm{Th} \rightarrow {}^{208}\mathrm{Pb} + 6^4\mathrm{He} + 4\mathrm{e}^- + 4\overline{\nu}_\mathrm{e} + 42.7\mathrm{MeV},$$
$$^{40}\mathrm{K} \rightarrow {}^{40}\mathrm{Ca} + \mathrm{e}^- + \overline{\nu}_\mathrm{e} + 1.32\mathrm{MeV}.$$

Since $\overline{\nu}_e$'s are detected in KamLAND via inverse β-decay, with a 1.8 MeV $\overline{\nu}_e$ energy threshold, KamLAND can detect geoneutrinos from ^{238}U and ^{232}Th. The radiogenic heat is generated in the decay chains inside the Earth. Based on the geophysical studies, it is known that the Earth's conductive heat flow has been evaluated to be 44.2 ± 1.0 TW [6] or 31 ± 1 TW [7] assuming much lower hydrothermal heat flow near mid-ocean ridges. On the basis of studies of chondritic meteorites, the calculated radiogenic power is thought to be 19 TW [8], and it is only about the half of the total heat flow. The radiogenic element abundance in the Earth's interiors (crust, mantle and core) deeply correlates with the Earth's geochemical and geophysical structures. So, the radiogenic power from the decay of ^{238}U and ^{232}Th is essential to understand the dynamics, formation and evolution of the Earth. According to the measurements of the concentrations of U and Th in the chondritic meteorites, the concentration mass ratio of Th to U inside the Earth is believed to be ~ 3.9 [9]. A reference model [10] was constructed using seismic data to divide the Earth into continental crust, oceanic crust, mantle, core and sediment, assuming that U and Th were absent from the core. According to the reference model, it was estimated that approximately 25% and 50% of the total geoneutrino flux originated within 50 km and 500 km of KamLAND, respectively.

KamLAND analyzed geoneutrinos based on data of a total detector live time of 749.1 ± 0.5 days collected from March 7 2002 to October 30 2004. The total exposure was $(7.09 \pm 0.35) \times 10^{31}$ target proton years, based on a fiducial volume with 5 m radius. The event selection cuts for the time difference (ΔT) and position difference (ΔR) between the positron and delayed neutron were $0.5\mu\mathrm{s} < \Delta T < 500\mu\mathrm{s}$ and $\Delta R < 1\mathrm{m}$, respectively. The efficiency for detecting geoneutrino candidates with energies between 1.7 and 3.4 MeV in the fiducial volume was estimated to be 0.687 ± 0.007. Figure 4 shows detected $\overline{\nu}_{\rm e}$ energy spectra in KamLAND. The dominant background sources for geoneutrino candidates were $\overline{\nu}_{\rm e}$'s from nuclear power reactors and the $^{13}{\rm C}(\alpha,{\rm n})^{16}{\rm O}$ reaction. The numbers of background events from reactor $\overline{\nu}_{\rm e}$'s and the $^{13}{\rm C}(\alpha,{\rm n})^{16}{\rm O}$ reaction were determined to be 80.4 ± 7.2 and 42 ± 11, respectively. The total background was estimated to be 127 ± 13 events including 2.38 ± 0.01 accidental coincidence events. On the other hand, the number of observed $\overline{\nu}_{\rm e}$ events was 152. Including the geoneutrino detection systematic errors, parts of which are correlated with the background estimation error, a rate only analysis gave 25^{+19}_{-18} geoneutrino candidates from the ^{238}U and ^{232}Th decay chains. Assuming a Th/U mass ratio of 3.9, estimated 90% confidence interval for the total number of ^{238}U and ^{232}Th geoneutrino candidates was 4.5 to 54.2. This result was consist with the central value of 19 predicted by geophysical models. The measurement of geoneutrinos, produced by the heat source in the Earth, means we obtain a new method for the research on the deep inside of the Earth and a new window into "Neutrino Geophysics" is opened.

4 Future prospects of observation of solar neutrinos

The coming topic of the KamLAND experiment is to study solar neutrinos with detection of low-energy solar neutrinos, such as ^{7}Be neutrinos ($E_\nu = 0.86$MeV). The measurement of the ^{7}Be neutrino flux can provide the verification of the SSM based on the high statistic. Moreover, KamLAND will observe the ^{8}B neutrino spectrum, which provides reconfirmation of the MSW effect in the solar neutrino oscillation, and the pep and CNO solar neutrino flux in real time, which was explored by R. Davis et al. as the first solar neutrino experiment. In the KamLAND detector, the solar neutrinos are detected via $\nu_{\rm e}$-e elastic scattering in real time, and it requires an ultra-low background environment. Figure 5 shows estimations of background based on the actual measurements in the current KamLAND scintillator. Although concentrations of the natural radioactivity of ^{238}U and ^{232}Th in the current KamLAND liquid scintillator are lower than the requirement from the solar neutrino measurement, the 5-6 orders of magnitude reduction is required for the ^{85}Kr impurities, 4-5 orders for the ^{210}Pb, and 2 orders for the ^{40}K. To achieve the requirements, a new liquid scintillator purification system has been developed and constructed in the detector site. It utilizes efficient purification methods of distillation, which

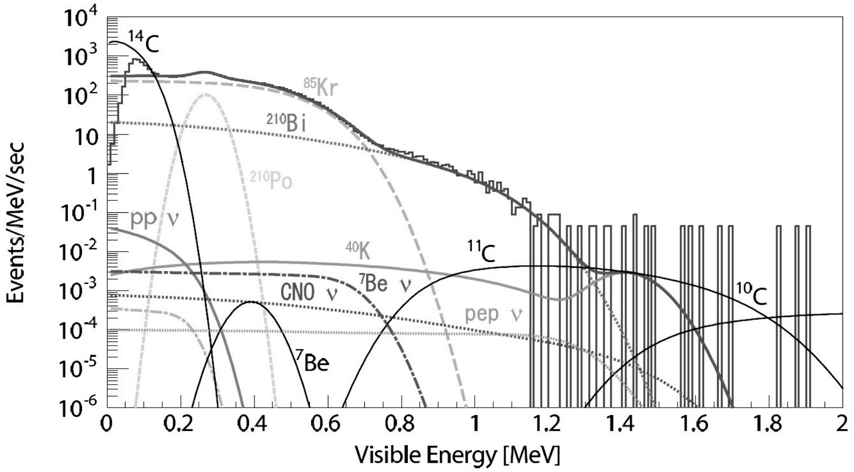

Figure 5: Current energy spectrum in KamLAND corresponding to a fiducial volume with 4 m radius.

separate substances based on differences in vapor pressures. Reduction rates of radionuclides obtained with test purification facilities are consistent with the requirements from the observation of the solar neutrinos. In addition to the purification of the liquid scintillator, seasonal variation of the ^{7}Be neutrino flux is useful for confirmation of solar neutrino signals and background estimation. On the other hand, recoil electrons interacting the pep or CNO neutrinos make a edge within 0.8-1.4 MeV. In this energy region, the dominant background is from the β-decays of ^{11}C ($\tau_{1/2} = 20.4$min) which are muon spallation products. However, approximately 95% of ^{11}C production reactions from ^{12}C produce neutrons and its efficiency is measurable with KamLAND. So, the background events from ^{11}C are efficiently rejected by the three-fold coincidence with muons, neutrons and the β's from ^{11}C. Although this analysis requires upgrade of electronics used with the detector to acquire the information of continuous reactions following muon events, KamLAND has the possibility of observation of the CNO cycle in the solar fusion reaction. The construction of the new purification system is going to be finished in this year, and purification of the liquid scintillator will be started. The solar neutrino observation in KamLAND is coming soon.

5 Conclusion

KamLAND has been studied neutrino physics involving neutrino geophysics and neutrino astrophysics. From the results of the reactor $\overline{\nu}_e$'s measurement, KamLAND showed the observed energy spectrum preferred the distortion expected from $\overline{\nu}_e$ oscillation effects and precisely measured neutrino oscillation parameters in 2005. And, an investigation of geoneutrinos in 2005 opened a new window for the exploration of the Earth. Search for the low energy solar neutrinos in KamLAND is in progress.

6 Acknowledgements

The KamLAND experiment is supported by the COE program under Grant No. 09CE2003 of the Japanese Ministry of Education, Culture, Sports, Science, and Technology, and under the United States Department of Energy Grant No. DEFG03-00ER41138. The reactor data are provided by courtesy of the following electric associations in Japan: Hokkaido, Tohoku, Tokyo, Hokuriku, Chubu, Kansai, Chugoku, Shikoku, and Kyushu Electric Power Companies, Japan Atomic Power Co., and Japan Atomic Energy Agency. The Kamioka Mining and Smelting Company has provided service for activities in the mine.

References

1. K. Eguchi *et al.* (KamLAND Collaboration), Phys. Rev. Lett. **90**, 021802 (2003).

2. T. Araki *et al.* (KamLAND Collaboration), Phys. Rev. Lett. **94**, 081801 (2005).

3. T. Araki *et al.* (KamLAND Collaboration), Nature **436**, 499-503 (2005).

4. K. Eguchi *et al.* (KamLAND Collaboration), Phys. Rev. Lett. **92**, 071301 (2004).

5. T. Araki *et al.* (KamLAND Collaboration), Phys. Rev. Lett. **96**, 101802 (2006).

6. H.N. Pollack, S.J. Hurter, J.R. Johnson, Heat flow from the Earth's interior: analysis of the global data set, Rev. Geophys. **31**, 267-280 (1993).

7. A.M. Hofmeister, R.E. Criss, Earth's heat flux revised and linked to chemistry, Tectonophysics **395**, 159-177 (2005).

8. W.F. McDonough, S.-s. Sun, The composition of the Earth, Chem. Geol. **120**, 223-253 (1995).

9. A. Rocholl, K.P. Jochum, Th, U and other trace elements in carbonaceous chondrites: Implications for the terrestrial and solar-system Th/U ratios, Earth Planet. Sci. Lett. **117**, 265-278 (1993).

10. S. Enomoto, Neutrino Geophysics and Observation of Geo-Neutrinos at KamLAND, Ph.D. thesis, Tohoku University (2005).